REPORT

20/2018
ISBN 978-82-7492-418-5
ISSN 2535-3004

Mapping of abandoned mine tailings and acid mine drainage using in situ hyperspectral measurements and WorldView-3 satellite imagery

Case study report

Author: CORINE DAVIDS

P.O. BOX 6434, TROMSØ SCIENCE PARK
N-9294 TROMSØ, NORWAY
TEL: +47 77 62 94 00, FAX: +47 77 62 94 01
post@norut.no
www.norut.no

PROJECT NAME: RESEM
Project No.: 602
CONTRACTING: Interreg Nord, Troms Fylkekommune
Contracting ref.:

Document No.: 20/2018
Document Type: Report
Status: Open
ISBN: 978-82-7492-418-5
ISSN: 2535-3004
No. of Pages: 16
Projectleader: Corine Davids
Date: 29.11.2018

Author: Corine Davids

Title: Mapping of abandoned mine tailings and acid mine drainage using in situ hyperspectral measurements and WorldView-3 satellite imagery

Summary:

This report describes the results of a preliminary analysis of very high resolution WorldView-3 satellite imagery for the detection and mapping of relatively small mine tailings and acid mine drainage associated to abandoned mines. In addition, ground-based hyperspectral images of the mine tailings and vegetation in contaminated and uncontaminated areas are used to extract spectral features in the visible and near infrared spectral range. The report will discuss the potential of using high and very high resolution satellite imagery to identify relatively small mine waste dumps and associated environmental effects in alpine environments.

Keywords: Optical remote sensing, SWIR, WorldView-3, mineral mapping, acid mine drainage

Notices: -

PUBLISHER: Norut, PO Box 6434, 9294 Tromsø, Norway

Contents

1 INTRODUCTION

Abandoned mines and mine tailings can cause long term environmental problems, such as acid mine drainage (AMD) and release of heavy metals in the environment. AMD is released from (underground) mines and mine tailings when sulphide minerals are exposed to water and oxygen and get oxidised. This oxidation process produces sulphuric acid, which dissolves heavy metals, such as Cu, Zn and As, in the rock and makes the drainage water both toxic and acidic. The resulting AMD can have a range of negative effects on, in particular, aquatic flora and fauna. When the pH of the acidic drainage water increases, e.g. through dilution with non acidic surface or groundwater, this leads to the precipitation of iron minerals such as iron sulphates, iron hydroxides and iron oxides. The accumulation of these precipitates cause a distinctive red staining of soil and rocks around AMD drainage (Fig.1).

Figure 1. Drainage and accumulation of iron precipitates around entrances near Nye Sulitjelma at ca 550 m altitude (left) and near Sulitjelma at ca 200 m altitude (right).

Since some of the most common precipitated minerals associated with AMD have distinctive spectral absorption features, remote sensing can be an efficient method to identify, map and monitor the locations of abandoned mines and mine tailings and the extent of AMD (Richter et al., 2008). It can complement conventional methods (through chemical analysis of soil/water samples) as it can put the findings in a more regional context and provide a better overview of quantities, sources and drainage pathways.

Several studies have investigated the use of satellite, airborne and ground-based remote sensing to detect and quantify geological materials (e.g. van der Meer et al., 2012; Sun et al., 2017), monitor environmental impacts (e.g. He et al., 2009), and mapping mine waste and AMD (Riaza et al., 2011; Kopačková et al., 2012; Mielke et al., 2014). The satellite data most frequently used for mineral remote sensing are multispectral ASTER data and hyperspectral Hyperion (decommissioned in 2017) data as these satellites include bands in the short wave infrared (SWIR) part of the spectrum. The SWIR bands are particularly useful for the discrimination of alteration minerals, such as those associated with AMD, which have only minor spectral differences in the visible to near infrared (VNIR) range. The spatial resolution of the ASTER and Hyperion data is 30 m (15 m for ASTER VNIR bands), which can make it challenging to detect smaller scale features. Airborne remote sensing from manned and unmanned aircrafts (Kopačková,

2012; Jackisch et al., 2018) is normally used to obtain higher spatial resolution in order to detect smaller features. However, in August 2014, the WorldView-3 satellite was launched by Digital Globe Inc. This commercial satellite includes 8 VNIR bands at 2 m spatial resolution, and 8 SWIR bands at 7.5 m spatial resolution, a significant improvement in both spatial and spectral resolution relative to the ASTER data and therefore well suited to distinguish different minerals at a smaller scale (Sun et al., 2017).

There has been mining activity at thousands of locations throughout Norway and there exist many abandoned mines (Miljødirektoratet, 2017a), often relatively small and in alpine environments. Mapping and monitoring of many of the smaller mining areas is limited (Miljødirektoratet, 2017b) and AMD from smaller mining areas is not well known.

The **objective** of this case study is to investigate to what extent WorldView3 VNIR and SWIR bands can be used to identify and map the spatial distribution of the mine tailings, the sources and pathways of acid mine drainage, and their impact on the vegetation. This case study is part of the EU Interreg Nord project 'REmote SEnsing supporting surveillance and operation of Mines (RESEM)', which aims to identify suitable remote sensing methods to help improve the design of mining structures and minimize the risks and environmental impact of mining in Arctic environments.

The case study will investigate the area around Sulitjelma in northern Norway, an area rich in sulphide deposits which have been mined for copper and zinc from 1886 to 1991. Since mine closure, minerals have been leaching from the abandoned mines and from deposited mine tailings and waste rock, and contaminated water runs into the nearby lake. As a company has expressed interest in reopening the mines, research into regional monitoring methods to identify and monitor mine related contamination, and the results of potential rehabilitation efforts is therefore highly relevant.

2 SITE DESCRIPTION

Sultitjelma is located in a mountainous region east of Bodø in northern Norway, at N67.1341 and E16.0849 (Fig. 2). Langvatnet, the main lake and lowest point in the area, lies at about 130 m altitude, while mining took place in the mountains around the lake up to altitudes of at least 800 m. The area is rich in sulphide deposits which have been mined for copper and zinc from 1886 to 1991. The mining was carried out mostly undergound in 18 different locations around Sulitjelma and Langvatnet (Fig. 2). In addition, there have been extensive exploration activities at ca 130 locations. This activity resulted in many but relatively small mine tailings scattered around the mountains.

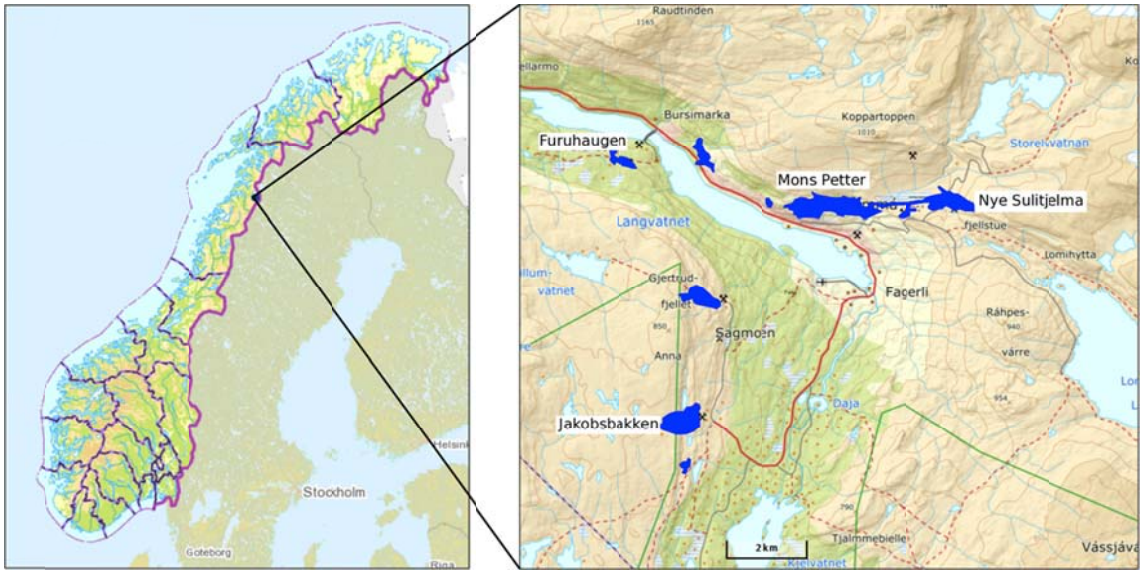

Figure 2. Location of Sulitjelma in Norway (left), and a topographic map of the area around Sulitjelma with the main ore deposits (modified after Kvennås et al., 2015).

A hundred years of copper and zinc mining in the alpine environment around Sulitjelma, in northern Norway, has resulted in significant heavy metal (Cu, Zn, As) contamination of Langvatnet due to AMD from the abandoned mine tunnels and deposited mine tailings.

It was estimated that more than 10 million tons of fine-grained processed waste (waste material from the metal extraction process in the smelter) was deposited in and around Langvatnet during operation of the mines and smelter. In addition, smaller amounts of mine tailings and waste rock were deposited around the mine entrances. Surface and groundwater draining from the mines and tailings supplied large amounts of Cu and Zn to Langvatnet; the annual supply of Cu and Zn to Langvatnet in 1991 was estimated at ca 50 tonnes of Cu and 47 tones of Zn.

After closure of the mines in 1991, many of the shafts and tunnels were filled with water in order to reduce the oxidation and leaching processes and reduce both the acidity of the surface and ground waters draining into Langvatnet, and the amount of Cu and Zn added.

3 DATA AND METHODS

3.1 SATELLITE DATA

A cloudless WorldView-3 satellite image was acquired on 22nd July 2017. The data was provided by ESA through their Third Party Mission Scheme. WorldView-3 is a commercial satellite by Digital Globe Inc. launched in August 2014, which includes 8 visible to near infrared (VNIR) bands at 2 m spatial resolution, and 8 short wave infrared (SWIR) bands at 7.5 m spatial resolution (Table 1). The SWIR bands are particularly useful for the discrimination of alteration minerals, which have only minor

spectral differences in the VNIR range. Previously, mineral detection and mapping was mostly done using ASTER satellite images; the ASTER data include similar SWIR bands, but at a lower spatial resolution of 30 m.

Table 1: Band set of WorldView 3

8 Multispectral Bands	wavelengths	8 SWIR Bands	wavelengths
Coastal:	400 - 450 nm	SWIR-1:	1195 - 1225 nm
Blue:	450 - 510 nm	SWIR-2:	1550 - 1590 nm
Green:	510 - 580 nm	SWIR-3:	1640 - 1680 nm
Yellow:	585 - 625 nm	SWIR-4:	1710 - 1750 nm
Red:	630 - 690 nm	SWIR-5:	2145 - 2185 nm
Red Edge:	705 - 745 nm	SWIR-6:	2185 - 2225 nm
Near-IR1:	770 - 895 nm	SWIR-7:	2235 - 2285 nm
Near-IR2:	860 - 1040 nm	SWIR-8:	2295 - 2365 nm

3.2 SATELLITE DATA PROCESSING

3.2.1 PRE-PROCESSING

The WorldView-3 data was delivered as level 2A, standard, for the VNIR bands and level 3D, orthorectified, for the SWIR bands. Both datasets were acquired at 22nd July 2017, 13:55 pm local time. Level 2A and 3D products are already corrected for radiometric and sensor distortions. Data (pre)processing and analysis was carried out using QGIS, OrfeoToolBox, Semi-Automatic Classification Plugin, and python 3 scripts. Data preprocessing is carried out according to Kuester et al. (2016) and Sun et al. (2017) and included the following steps: 1. Radiometric calibration to convert the digital numbers into top-of-atmosphere (TOA) spectral radiance; 2. Conversion from TOA spectral radiance to TOA spectral reflectance by correcting for solar irradiance and solar angle; 3. Conversion to top-of-canopy (TOC) spectral reflectance by correcting for the effect of the atmosphere using a simple atmospheric correction model; and 4. Creating masks for vegetation, snow, clouds and water.

Both level 2A and 3D data were first converted to TOA spectral radiance L according to following equation:

$$L = GAIN \times DN \times \frac{absCalFactor}{effectiveBandwidth} + OFFSET \quad (1)$$

Where L is at sensor radiance in (W m^{-2} sr^{-1} μm^{-1}), absCalFactor and effectiveBandwidth (μm) are found in the .IMD file and GAIN and OFFSET values are found in Digital Globe's technical note 'Radiometric Use of WorldView-3 Imagery' by Kuestner (2016).

The TOA radiance was then converted into TOA reflectance, $\rho(TOA)_{\lambda}$ according to equation 2:

(2) $$\rho(TOA)_\lambda = \frac{L_\lambda d^2 \pi}{E_\lambda cos\theta_S}$$

Where L_λ is the at-sensor radiance for spectral band λ, d is the Earth-Sun distance in astronomical units; E_λ is the band-averaged solar exoatmospheric irradiance; and θ_S is the solar zenith angle (Kuestner, 2016).

Further atmospheric correction and conversion to top-of-canopy (TOC) reflectance was carried out using the OrfeoToolBox, which uses the 6S radiative transfer model to model the effect of the atmosphere.

For the VNIR dataset, a vegetation mask was created based on the Normalised Difference Vegetation Index (NDVI), which gives and indication of greenness, using a threshold value of >0.5. The NDVI was calculated based on the standard equation, using band 7, near-IR1, for NIR, and band 5 for red:

(3) $$NDVI = \frac{NIR - red}{NIR + red}$$

A snow and cloud mask was created based on band 1 with a threshold value of 0.4. A water mask was created based on zero values in red and NIR bands 5-8. The vegetation, snow and cloud, and water masks were then combined into one final mask.

Ideally, the two datasets, VNIR and SWIR data, should be stacked and analysed together. However, the two datasets were delivered with different levels of orthorectification (level 2A is projected to a constant base elevation, while level 3D is orthorectified with a DEM), which causes an offset between the datasets. Due to the limited time available for this case study, it was decided to analyse the datasets separately. Further orthorectification to the same level, resampling to the same spatial resolution and joint analysis was not possible within this project and will be done at a later stage.

3.2.2 ANALYSIS – ALTERATION INFORMATION EXTRACTION

There are a number of analytical techniques to extract spectral features from multispectral data. When lacking in situ data, mineral indices or simple band ratios can be applied to enhance certain spectral features (e.g. Sun et al., 2017). In addition, techniques to enhance the variation in a dataset, such as principal component analysis (PCA), can be used to emphasize spectral differences. If, however, in situ data is available and mineral spectra are known, techniques such as spectral angle mapping (SAM), spectral feature fitting (SFF) or spectral mixture analysis (SMA) can be used to detect and map the probability of presence of certain minerals (Kopačková, 2014, and references herein). In this study, only limited in situ data was available, and we investigated to what extent simple band ratios, mineral indices and PCA analysis with thresholds can be used to extract information on abandoned mines and mine tailings.

Sun et al., (2017) proposed, amongst others, the following index:

Fe-OH index = (SWIR-3/SWIR-7) * (SWIR-3/SWIR-1)

In addition, band ratios VNIR-5/VNIR-3, VNIR-8/VNIR-6, SWIR-1/SWIR-3, and SWIR-3/SWIR-7 were investigated. PCA analysis was carried out on both VNIR band set and the SWIR band set separately. Results of the analysis were visually compared to the data, and to photos and field notes taken at known locations in the field.

3.3 IN SITU HYPERSPECTRAL DATA COLLECTION AND PROCESSING

Ground-based hyperspectral imaging, using a Rikola hyperspectral camera (500-900nm), was carried out from 28-31 July 2017 to collect in situ measurements of mine waste, vegetation and soil in contaminated areas and healthy alpine vegetation. The camera was programmed to collect 39 bands between 500-900 nm (visible to NIR) with spectral widths of 10-15 nm, covering the full spectrum. The Rikola camera was placed on a tripod and measurements were taken straight down, at nadir position, to avoid any directional influence and make it easier to compare with satellite data. Prior to each measurement, a dark background image was collected and an image of 3 grey reflectance panels (Fig. 3).

Figure 3. Set-up for in situ hyperspectral measurements with Rikola camera (left). Reflectance calibration panels (right).

Pre-processing of the data included camera calibration and dark background subtraction to convert the raw data to radiance, image band coregistration, and empirical line calibration using the grey reflectance panels to convert radiance to reflectance. Spectral data of target objects were obtained by manually outlining the object of interest (soil, plant etc.) and calculating the average reflectance values. The in situ hyperspectral data was used to extract spectral characteristics in the VNIR range from different plant species, moss and different types of waste rocks for end member determination and validation.

4 RESULTS AND DISCUSSION

4.1 IN SITU HYPERSPECTRAL DATA

Figure 4 shows the spectra of selected objects, including two types of sedges (*Carex* species), which are some of very few plants that grow on iron crusted soils in this area. Figure 5 shows some examples of the surface and objects measured with the hyperspectral camera.

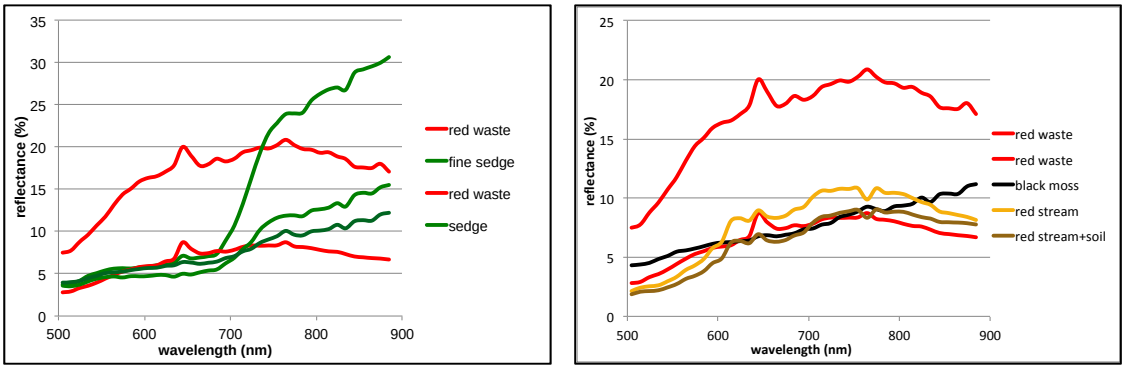

Figure 4. Examples of different spectra from vegetation growing in contaminated areas, iron crusted soil, soil with dark moss, and a small stream with iron precipitation.

Figure 5. Examples of surfaces measured. Sedge growing on iron crusted soil (left), mine tailings (right).

The spectra from iron crusted rocks and mine tailings (red waste) show a sharp peak around 650 nm (red) and a broad peak around 760 nm. The spectra are used to identify which bands or spectral ranges in the VNIR range can be used to distinguish different objects of interest. At a later stage, these spectra can also be used as part of supervised classification and spectral matching methods (such as SAM, SFF, SMA; see 4.2.2), but this could not be achieved within this study.

4.2 WORLDVIEW-3 SATELLITE DATA

Figure 6 shows the WorldView-3 VNIR and SWIR images of the area between Sulitjelma, at the lake Langvatnet, and the Nye Sulitjelma mines in the mountains above Sulitjelma.

For the VNIR band set, the best results were obtained with the band ratio VNIR-8/VNIR-6 (Figs. 7-10). This is related to the observation that the peak of the iron crust spectra is located around 760 nm (Fig. 4), and VNIR-6 band is the narrow band closest to this peak. Figure 7 shows that the mine tailings near the Nye Sulitjelma mines, iron crusted rocks along the AMD drainage, and the gravel area around the processing plant are clearly outlined. The gravel road from Sulitjelma into the mountains to the Nye Sulitjelma mines is also partially highlighted in red. This is to be expected as the gravel surface is crushed country rock; the crushing has increased the exposed surface area and weathering processes can also lead to some degree of iron crust formation depending on the country rock's mineralogy. However, the asphalt road in Fig. 10 and some of the rocky outcrops in the mountains (Fig. 7) are also outlined in red, indicating some degree of overestimation, but without ground data for validation it is difficult to say to what extent. Iron crusts do also form naturally through weathering of iron rich rocks.

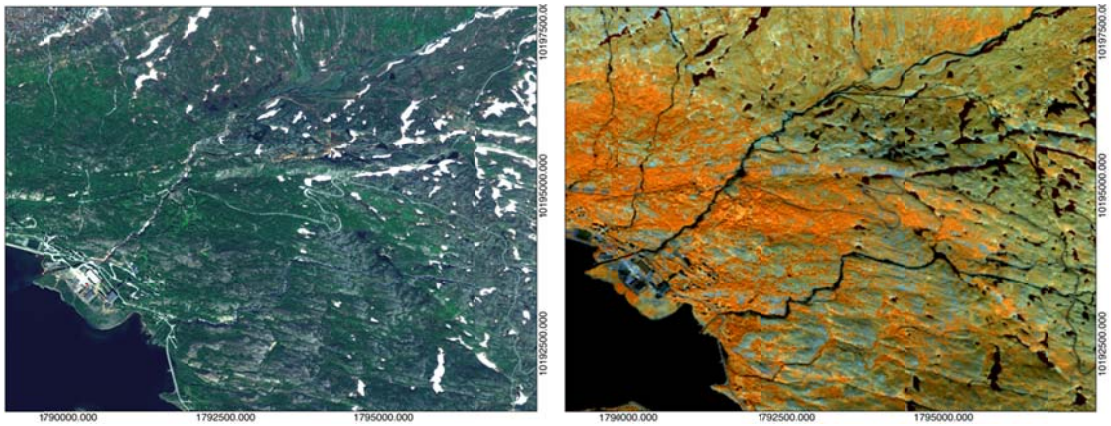

Figure 6. WorldView-3 VNIR image with bands 5, 3, and 2, and 2.5 m spatial resolution showing the area around Sulitjelma, with Langvatnet and the abandoned processing plant in the bottom left, the road up to the mines at Nye Sulitjelma and some of the mining areas with mine tailing (reddish colour top right). Bottom image is the WorldView-3 SWIR image with bands 1, 3, and 7, and a spatial resolution of 7.5 m. Blue-ish colours indicate bare rock and mine tailings, reddish is vegetation.

For the SWIR band set, the band ratio SWIR-1/SWIR-3 gives the best results, similar to VNIR-8/VNIR-6 (Figs. 7-10). This band ratio is based on the observation that ferrous ions have an absorption feature in the wavelengths of SWIR-1 (Sun et al., 2017). Also here there appears some overestimation in areas with bare rock, but without obvious mine tailings, which could be related to weathering. The SWIR-1/SWIR-3 band ratio gives better results than the Fe-OH index.

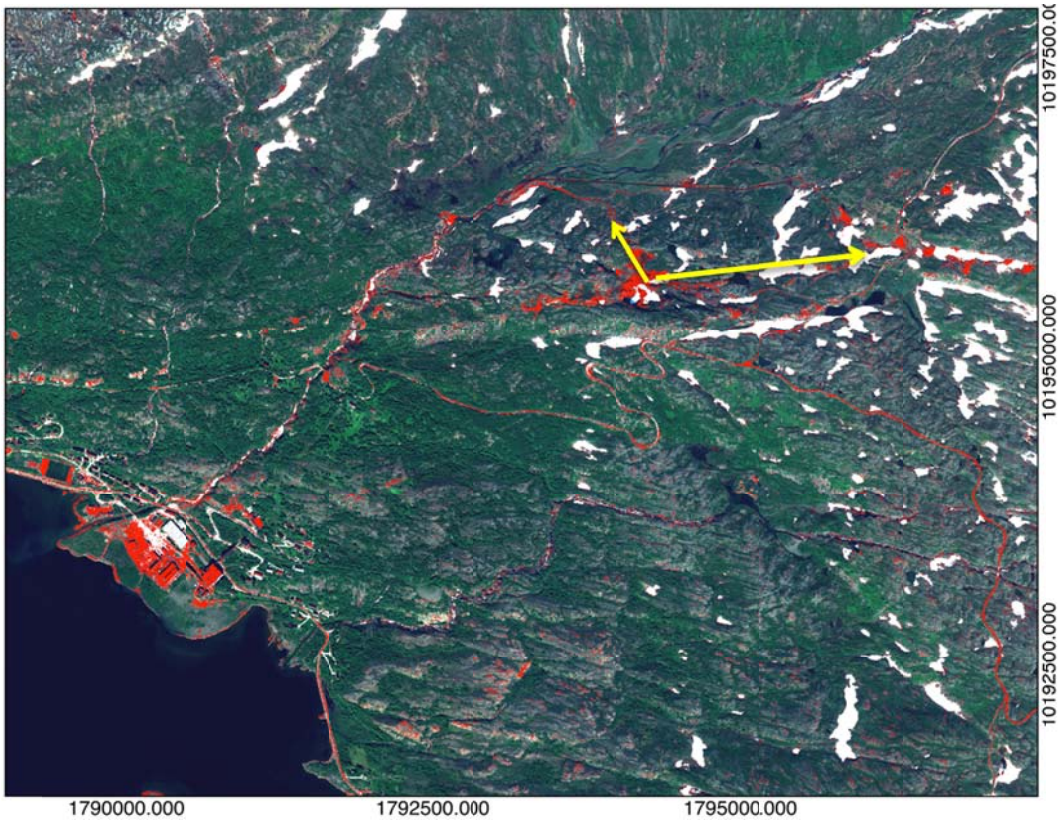

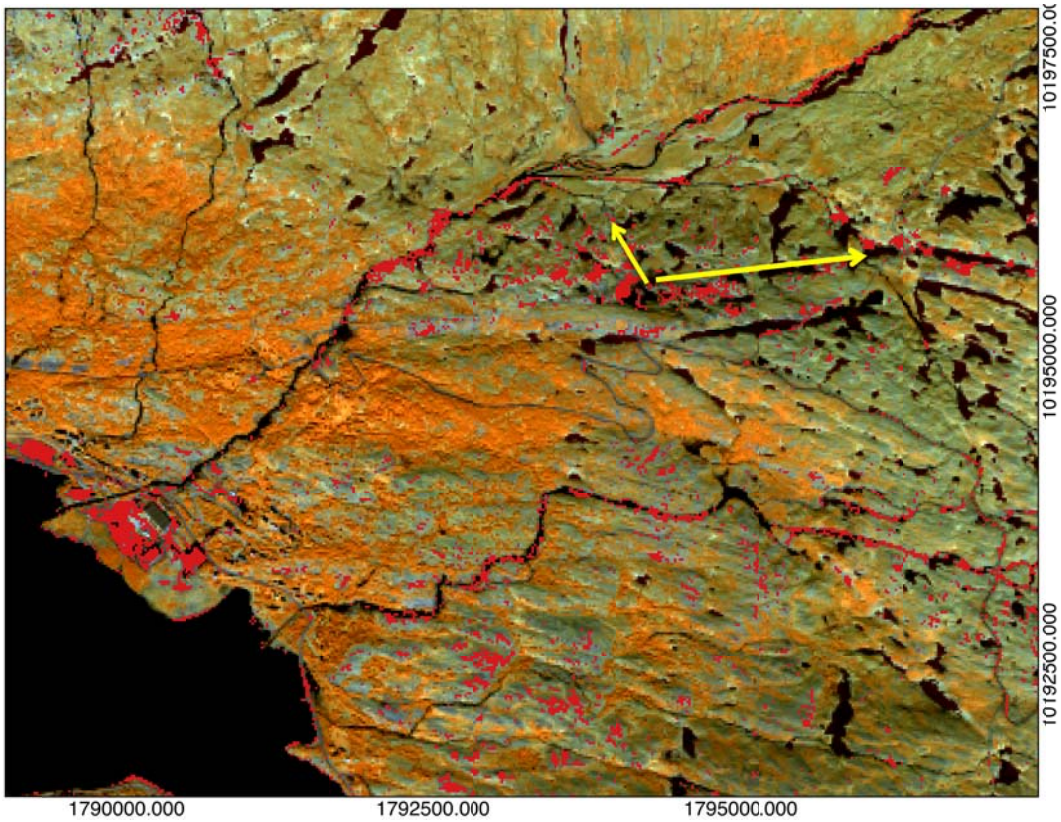

Figure 7. Top: WorldView-3 VNIR image as base image (Fig. 6 for details). Overlain in red is the result from the band ratio VNIR-8/VNIR-6, with a threshold at 0.9. Bottom: WorldView-3 SWIR image as base image (Fig. 6) with overlain in red the results from the band ratio SWIR-

1/SWIR-3, with a threshold of 0.75. Yellow arrows give the location and direction of the photos in Fig. 8.

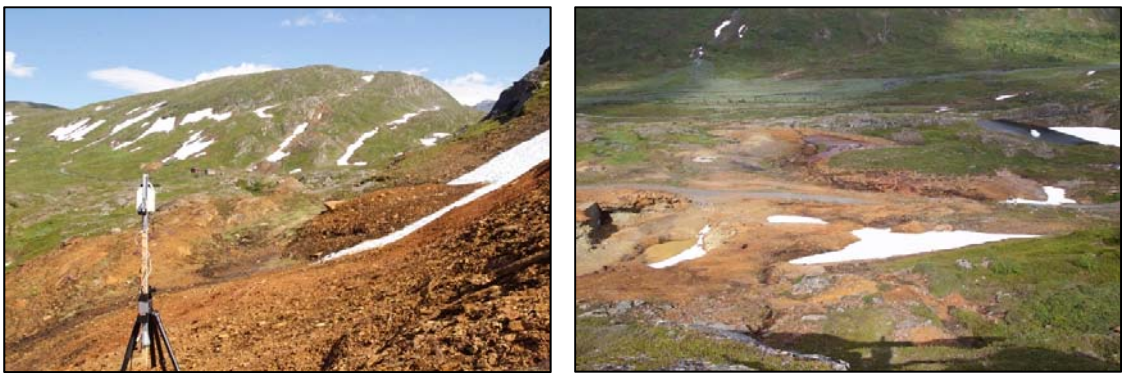

Figure 8. Two photos taken along the yellow arrows in Fig. 7. Bottom left: View to the east; bottom right: view to the northwest.

Figure 9. The 2 photos are taken along the yellow arrows in Fig. 10. Left: View to the west; right: view to the east.

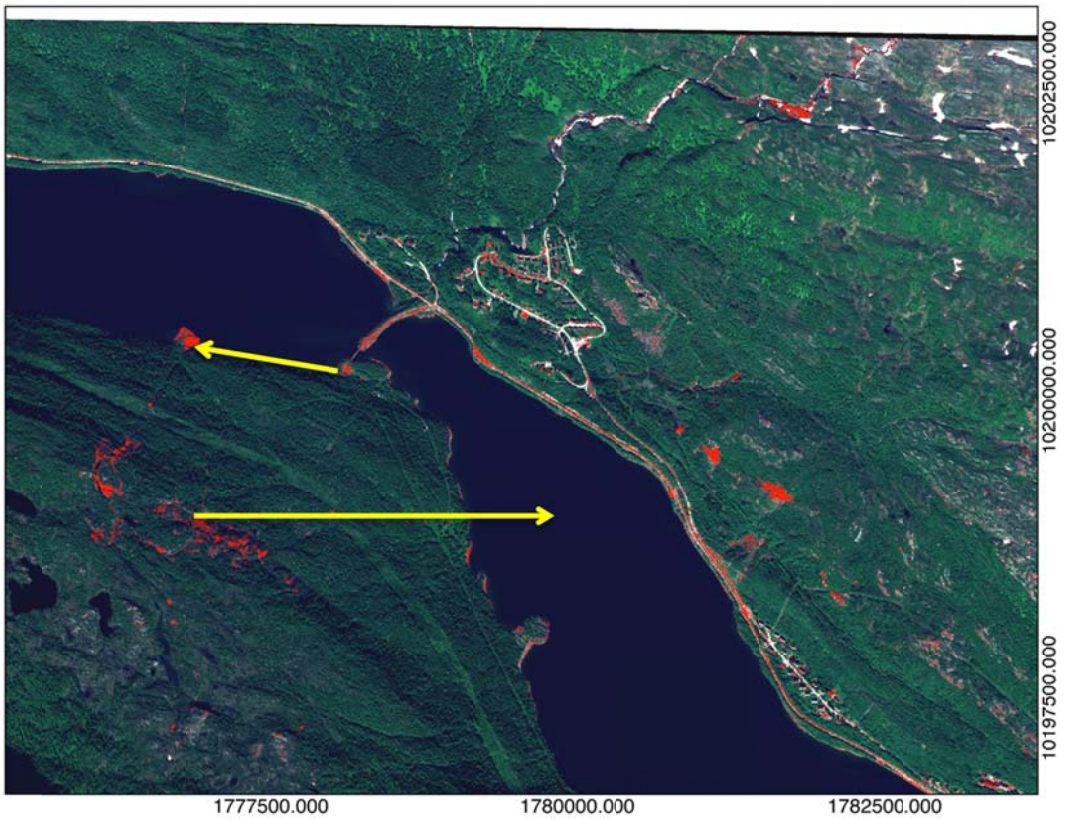

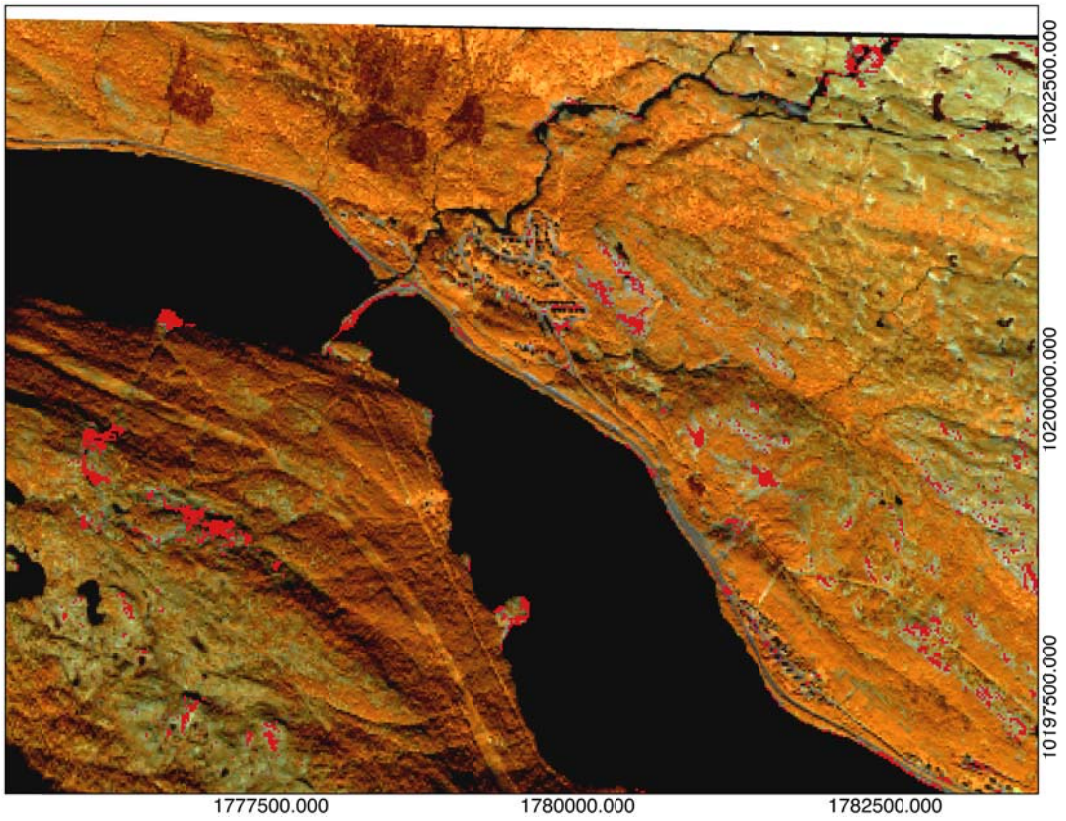

Figure 10. Another example mapping mine tailings around the western part of Langvatnet, west of Sulitjelma. Same band combinations and band ratios as in Figs. 6 and 7. Yellow arrows indicate the location and direction of the photos in Fig. 9.

5 CONCLUSIONS

This report presents the results of a preliminary analysis of WorldView-3 VNIR and SWIR satellite data to map mine tailings and AMD drainage patterns. The results in 5.2 show that even simple band ratios combined with thresholding can give a good first overview of the areas that most likely contain mine tailings and/or iron mineral precipitation associated with AMD.

The results in this study indicate that the VNIR bands can also be used to create an overview map of mine tailings and AMD. Particularly VNIR-6, which is associated with a minor peak in the iron crust spectrum, is useful. This suggests that the freely available Sentinel-2 satellite data, which includes a red edge band, band 6, with a similar spectral range as WorldView-3 VNIR-6, could be used for the mapping of mine tailings and AMD. The spatial resolution of Sentinel-2 is, however, lower at 10-20 m. For smaller mining areas it may therefore be necessary to purchase higher resolution commercial satellite data or use airborne or droneborne multispectral or hyperspectral imaging.

Combining VNIR and SWIR data and using more advanced methods such as SAM or SMA, is expected to further improve detection and mapping of mine tailings and AMD. For the latter, spectral data from either in situ or laboratory measurements, or spectral libraries are needed.

Similar methods can be used to detect problems with e.g. vegetation health, or map biomass as index for biodiversity (possible link to groundwater upwelling).

6 REFERENCES

He, B., Oki, K., Wang, Y., Oki, T., 2009. Using remotely sensed imagery to estimate potential annual pollutant loads in river basins. Water Science and Technology, 60/8: 2009–2015.

Jackisch, R., Lorenz, S., Zimmermann, R., Möckel, R., and Gloaguen, R., 2018. Drone-Borne Hyperspectral Monitoring of Acid Mine Drainage: An Example from the Sokolov Lignite District. Remote Sensing, 10, 385. doi:10.3390/rs10030385

Kopačková, V., 2014. Using multiple spectral feature analysis for quantitative pH mapping in a mining environment. International Journal of Applied Earth Observation and Geoinformation, 28: 28-42.

Kopačková, V., Chevrel, S., Bourguignon, A., and Rojík, P., 2012. Application of high altitude and ground-based spectroradiometry to mapping hazardous low-pH material derived from the Sokolov open-pit mine. Journal of Maps, 8:3: 220-230. DOI: 10.1080/17445647.2012.705544

Kvennås. M., Okkenhaug, O., Lundgren, T., and Ambiental, 2015. Sulitjelma gruver: vurdering av mulige tiltaksalternativ. NGI rapport 20140315-R-03.

Kuester, M., 2016. Technical Note: Radiometric use of WorldView-3 Imagery. DigitalGlobe 22.2.2016.

van der Meer, F.D., van der Werff, H.M.A., van Ruitenbeek, F.J.A., Hecker, C.A., Bakker, W.H., Noomen, M.F., Van der Meijde, M., Carranza, E.J.M., de Smeth, J.B., and Woldai, T., 2012. Multi- and hyperspectral geologic remote sensing: a review. International Journal of Applied Earth Observation and Geoinformation, 14: 112–128.

Mielke, C., Boesche, N.K., Rogass, C., Kaufmann, H., Gauert, C., and de Wit, M., 2014. Spaceborne Mine Waste Mineralogy Monitoring in South Africa, Applications for Modern Push-Broom Missions: Hyperion/OLI and EnMAP/Sentinel-2. Remote Sensing, 6: 6790–6816.

Miljødirektoratet, 2017a. Avrenning av tungmetaller fra nedlagte kisgruver. http://www.miljostatus.no/tema/ferskvann/miljogifter-i-ferskvann/avrenning-av-tungmetaller-fra-nedlagte-kisgruver/, 09.05.2017.

Miljødirektoratet, 2017b. Mindre kisgruver. http://www.miljostatus.no/tema/ferskvann/miljogifter-i-ferskvann/avrenning-av-tungmetaller-fra-nedlagte-kisgruver/mindre-kisgruver/Rapport. 24.05.2017.

Riaza, A., Buzzi, J., García-Meléndez, E., Carrère, V., and Müller, A., 2011. Monitoring the Extent of Contamination from Acid Mine Drainage in the Iberian Pyrite Belt (SW Spain) Using Hyperspectral Imagery. Remote Sensing, 3: 2166–2186.

Richter, N., Staenz, K., and Kaufmann, H., 2008. Spectral unmixing of airborne hyperspectral data for baseline mapping of mine tailings areas. International Journal of Remote Sensing, 29/13: 3937-3956.

Sun, Y., Tian, S., and Di, B., 2017. Extracting mineral alteration information using WorldView-3 data. Geoscience Frontiers 8: 1051-1062.